JACS
JOURNAL OF THE AMERICAN CHEMICAL SOCIETY

Communication

pubs.acs.org/JACS

Development of a Selective Chemical Etch To Improve the Conversion Efficiency of Zn-Rich Cu_2ZnSnS_4 Solar Cells

Andrew Fairbrother,[†] Eric García-Hemme,[†] Victor Izquierdo-Roca,[†] Xavier Fontané,[†] Fabián A. Pulgarín-Agudelo,[‡] Osvaldo Vigil-Galán,[§] Alejandro Pérez-Rodríguez,[†,∥] and Edgardo Saucedo*[,†]

[†]IREC, Catalonia Institute for Energy Research, C. Jardins de les Dones de Negre 1, 08930 Sant Adrià del Besòs, Barcelona, Spain

[‡]Centro de Investigación en Energía-UNAM, 62580 Temixco, Morelos, Mexico

[§]Escuela Superior de Física y Matemáticas, Instituto Politécnico Nacional, C.P. 07738, México D.F., Mexico

[∥]IN2UB, Departament d'Electrònica, Universitat de Barcelona, C. Martí i Franquès 1, 08028 Barcelona, Spain

Supporting Information

ABSTRACT: Improvement of the efficiency of Cu_2ZnSnS_4 (CZTS)-based solar cells requires the development of specific procedures to remove or avoid the formation of detrimental secondary phases. The presence of these phases is favored by the Zn-rich and Cu-poor conditions that are required to obtain device-grade layers. We have developed a selective chemical etching process based on the use of hydrochloric acid solutions to remove Zn-rich secondary phases from the CZTS film surface, which are partly responsible for the deterioration of the series resistance of the cells and, as a consequence, the conversion efficiency. Using this approach, we have obtained CZTS-based devices with 5.2% efficiency, which is nearly twice that of the devices we have prepared without this etching process.

Two years ago, with the challenging demonstration of a 9.7% efficiency $Cu_2ZnSn(S,Se)_4$ (CZTSSe)-based solar cell,[1] interest in these materials began to increase rapidly. CZTSSe, also commonly referred to as kesterites because of their crystal structure, are currently the most promising materials to replace $Cu(In,Ga)(S,Se)_2$ (CIGS) absorbers in photovoltaic devices in the mid- to long-term, anticipating potential limitations for mass production of CIGS-based technologies in the coming years due to the scarcity of In and Ga.[2,3] Kesterites have the advantage that they are formed by abundant or cheap and low-toxicity elements, with a direct band gap tunable between 1.0 and 1.5 eV (from pure Se to pure S compounds). In addition, they exhibit p-type conductivity and have a high light absorption coefficient, up to 1 order of magnitude higher than for CIGS, suggesting that devices with reduced thickness could function efficiently.[4] Even though the current highest efficiency values have been obtained for films with a significant Se content,[1,5] targeting a Se-free Cu_2ZnSnS_4 (CZTS)-based device is still interesting because of the lower cost of S and the lower toxicity of sulfide-related compounds compared to selenide ones. This gives motivation for the further development and optimization of CZTS-based technologies using processes compatible with scale-up to industrial and mass production levels.

Despite the promising qualities of CZTS, the maturity of kesterite-based technologies is still low, and, aside from their intrinsic peculiarities, most of the processes required to obtain the current highest efficiency devices are identical to previous CIGS technology.[1,6,7] One of the most interesting results in kesterite research is that the best efficiencies have been obtained using absorbers synthesized by means of liquid-phase methods, as opposed to the vapor-phase methods that are required for the highest efficiency CIGS devices.[1,8] A significant amount of work has been carried out to understand the physical mechanisms limiting the efficiency of CZTS solar cells fabricated using vapor-phase methods, and it has been established that Sn loss at temperatures >400 °C is one of the main limiting features during processes involving high temperatures.[7] A remarkable increase in the conversion efficiency was reported when samples were thermally treated in a Sn-containing atmosphere. As additional evidence, the decomposition of CZTS has been clearly observed when samples were heated at 560 °C in vacuum during 6 h, confirming the loss of Sn under Sn- and S-deficient atmospheric conditions.[7]

Almost all CZTS solar cells that exhibit efficiency >3% have been prepared under Cu-poor and Zn-rich conditions.[1,5,7−10] The most common compositional ranges are Cu/(Zn+Sn) ratio between 0.80 and 0.95 and Zn/Sn ratio between 1.10 and 1.25.[1,5,7−10] These ratios prevent the formation of low band gap ternary phases (with Cu−Sn−S, for example Cu_2SnS_3) which are favored in Cu-rich conditions and are considered responsible in large part for the low V_{OC} of devices prepared in such conditions. Due to the Zn excess in the best devices, Zn-rich secondary phases are expected, and in fact the presence of ZnS(Se) phases in CZTS(Se) films has been confirmed by Raman spectroscopy measurements.[11,12] However, to date no specific procedures have been adopted for the selective removal of these phases, and the classical KCN-based etching for the selective removal of Cu-rich phases such as Cu_xS_y and Cu_xSe_y,[13,14] initially developed for CIGS technologies, is still widely used in published works about CZTS.[1,6,7] In our experience, the solubility of ZnS in KCN solutions (up to KCN 10% m/v) is practically negligible.

Received: February 10, 2012
Published: April 30, 2012

dx.doi.org/10.1021/ja301373e | J. Am. Chem. Soc. 2012, 134, 8018−8021

Some alternative etching procedures have been explored, but with limited improvement in device properties reported. One notable exception is the H_2O etching used by Katagiri to remove superficial oxide phases, leading to an improvement in efficiency from 5.74% to 6.77%.[10] Timmo and Mellikov used Br-MeOH, NH_4OH, and HCl as etchants on CZTS monograins with Zn-poor surfaces,[15,16] and Maeda used HCl on films prior to CdS deposition but did not discuss its purpose or effects.[17] The effectiveness of HCl at removing Zn-rich phases has been evidenced indirectly in some works but not explored in detail. For example, Platzer-Björkman and Scragg showed compositional depth profiles with Zn-poor surface regions in cells that were etched short times with HCl to remove the window layer for analysis,[9,18] and Lauermann noted the solubility of ZnS in HCl at room temperature but with etch times of several hours.[19]

In this Communication, we present an alternative chemical etching procedure based on hydrochloric acid solutions that has been developed for the selective removal of Zn-rich secondary phases, and we show its effectiveness in improving solar cell conversion efficiency. With this aim, we have prepared Zn-rich and Cu-poor CZTS-based solar cells by a two-stage process, involving the deposition of Sn/Cu/Zn metallic stacks by means of DC-magnetron sputtering onto Mo-coated soda-lime glass substrates, followed by reactive annealing under a sulfur- and tin-containing atmosphere. The composition ratios of the precursor stack as measured by X-ray fluorescence spectroscopy (XRF) are Cu/(Zn+Sn) = 0.73 and Zn/Sn = 1.27, while the sulfurized samples before etching have ratios of Cu/(Zn+Sn) = 0.80 and Zn/Sn = 1.55, the difference being due to Sn loss during annealing. The composition ratios after 300 s of etching in HCl (5% v/v, 75 °C) are Cu/(Zn+Sn) = 1.00 and Zn/Sn = 1.15. The effects of HCl concentration and etch time are described in more detail in the Supporting Information (SI).

After etching of the absorbers, glass/Mo/CZTS/CdS/ZnO(i)/ZnO(Al) cells were produced by chemical bath deposition of the CdS buffer layer, followed by two-stage sputtering deposition of the ZnO layers (see the SI for experimental details).

Figure 1 shows the Raman spectra measured with 325 nm (UV) excitation wavelength (blue spectra) and 514 nm excitation wavelength (red spectra) from the as-grown sample (curves labeled (a)) and from the samples etched with the HCl solution (curves labeled (b) and (c)). The spectrum measured from the as-grown sample with the UV excitation wavelength is dominated by three intense peaks at 348, 696, and 1044 cm^{-1}, which are identified as the first-, second-, and third-order peaks characteristic of the ZnS phase.[11] The high intensity of these peaks is due to the existence of a quasi-resonant excitation of the ZnS vibrational modes at these excitation conditions, in which Raman spectroscopy becomes extremely sensitive in the detection of even small quantities of ZnS in the sample.[11] This spectrum also shows a contribution at 338 cm^{-1} (appearing as a shoulder at the low-frequency side of the dominant first-order ZnS peak) and a weaker peak at 287 cm^{-1} which correspond to the main A1 modes characteristic of the CZTS phase.

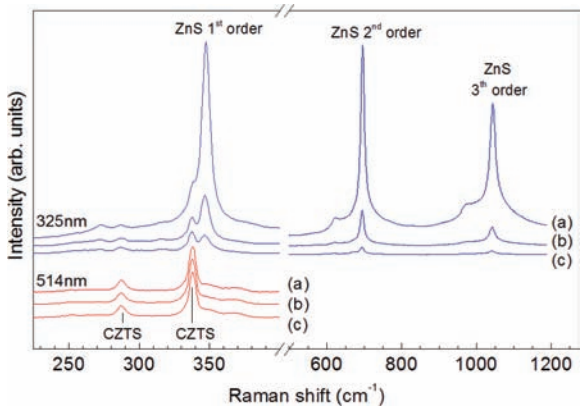

Figure 1. Raman spectra taken for the as-grown sample (a), sample etched with a solution of HCl (5% v/v) at 75 °C for 90 s (b), and sample etched with HCl solution (5% v/v) at 75 °C for 300 s (c). Excitation wavelengths: 325 nm (blue spectra), 514 nm (red spectra).

After chemical etching with a solution of HCl (5% v/v, 75 °C, 90 s), the intensity of the ZnS Raman peaks is drastically reduced (Figure 1, blue spectrum (b)), and for longer etching times (300 s, Figure 1, blue spectrum (c)) the ZnS Raman peaks are reduced even more. In contrast, under equivalent measurement conditions, the Raman peaks corresponding to CZTS remain unaffected, in both their intensity and spectral features (frequency, width). This suggests that the proposed chemical etching does not significantly affect the kesterite surface. To confirm this, the same analysis was made using a 514 nm excitation wavelength, which is well suited for analysis of the dominant kesterite phase (see red spectra in Figure 1). No significant changes in the spectra from the different samples are observed, confirming that the proposed etching procedure does not significantly affect the CZTS surface. It is important to remark that sample etched by the classical KCN route (aqueous solution 10% m/v, 25 °C, 120 s) does not show any significant difference in the Raman spectra measured with both excitation wavelengths in comparison with the as-grown sample, confirming the ineffectiveness of this procedure to eliminate the ZnS secondary phase.

This agrees with the measurements that we performed on the solubility of 20 mg of some potential secondary phases of the system both in 20 mL of a KCN solution (aqueous solution 10% m/v, 25 °C, 120 s) and in an HCl solution (aqueous solution 5% v/v, 75 °C, 300 s). For the KCN etching we obtained the following results: CuS, completely soluble; ZnS, insoluble; and SnS, insoluble. For the HCl etching we obtained the following results: CuS, insoluble; ZnS, completely soluble; and SnS, slightly soluble. This chemical approach supports the high selectivity of our proposed etching process for the ZnS binary phase. It is important to note that the solubility of Sn-rich phases in HCl is noted by Timmo, Mellikov, and Li in CZTS,[15,16,20] but the presence of SnS in Zn-rich films tends to be related to peculiarities of that specific system, i.e., a Sn-rich surface or localized SnS phase formation due to Sn layer nonuniformity. In fact, by using inductively coupled plasma mass spectroscopy (ICP-OES), we estimate that the solubility of ZnS is ~2 orders of magnitude greater under similar dissolution conditions than that of SnS (see SI for more details). Also, we analyzed the supernate after the etching marked as (c) in the Figure 1, obtaining the following composition results: [Zn], 0.4 ppm; [Cu] and [Sn], not detected. This compositional analysis supports the observed insolubility and low solubility of CuS and SnS in HCl respectively.

The distribution of the ZnS secondary phase on the surface of the samples and its dependence on the etching processes have also been investigated by Raman scattering mapping measurements performed under UV excitation conditions.

dx.doi.org/10.1021/ja301373e | J. Am. Chem. Soc. 2012, 134, 8018–8021

Figure 2A shows an optical image on the surface of the as-grown sample, where dark areas correspond to ZnS-rich regions

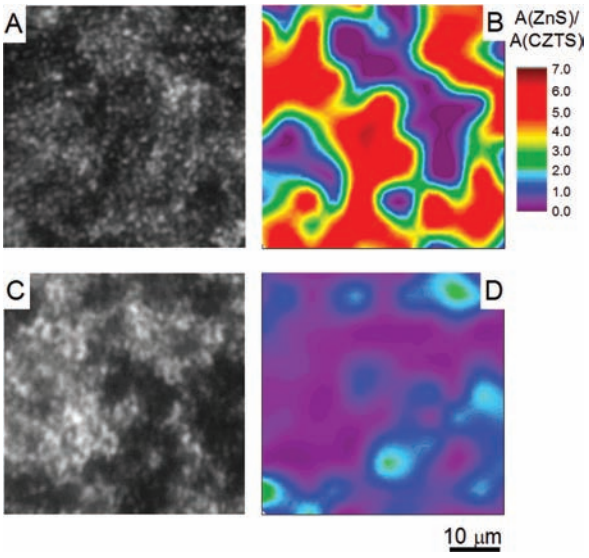

Figure 2. Optical image of the as-grown sample (A) and UV Raman mapping in the same area, representing the ratio between the intensity of the main ZnS Raman mode at 348 cm^{-1} and that of the main CZTS A1 mode at 338 cm^{-1} (B). Optical image of the sample etched with the solution of HCl (5% v/v, 75 °C) for 300 s (C) and UV Raman mapping in the same area, representing the ratio between the intensity of the main ZnS Raman mode at 348 cm^{-1} and that of the main CZTS A1 mode at 338 cm^{-1} (D).

and white areas to CZTS-rich regions. The UV Raman mapping in Figure 2B shows in a color code the ratio between the intensity of the main ZnS Raman peak at 348 cm^{-1} and that of the main A1 CZTS mode at 338 cm^{-1}, with red areas corresponding to regions with high ZnS content and violet areas corresponding to regions with low ZnS content. This Raman mapping correlates strongly with the optical image, showing the nonuniform distribution of ZnS on the surface, similar to the distribution of Cu_xS in CIGS.[14] After the etching process with an HCl-based solution, a drastic reduction of the black areas in the optical image is clearly seen, as well as corresponding changes in the UV Raman mapping. The ZnS phase is practically eliminated from the entire sample surface, with only residual quantities of ZnS found in certain places. This is a very important result, because for the first time we shown unambiguously the effectiveness of this selective etching for the elimination of ZnS.

An additional proof of concept for the presented chemical etching process is reflected in its effect on the optoelectronic parameters of the cells made with the different absorbers. Figure 3 shows the illuminated $J-V$ characteristics of the solar cells prepared with three different absorber layers: the as-grown layer, that obtained after the classical KCN etching, and that obtained after our novel HCl-based etching. Comparing the optoelectronic parameters, the classical KCN etching gives limited improvement to the results obtained from the unetched (as-grown) sample. The conversion efficiency is improved slightly, from 2.7% to 3.3%, as presented in the table shown in Figure 3. In contrast, the largest improvement on the optoelectronic parameters is achieved when the HCl-based etch is applied to the samples, giving solar cells with 5.2% conversion efficiency. This improvement is clearly seen over

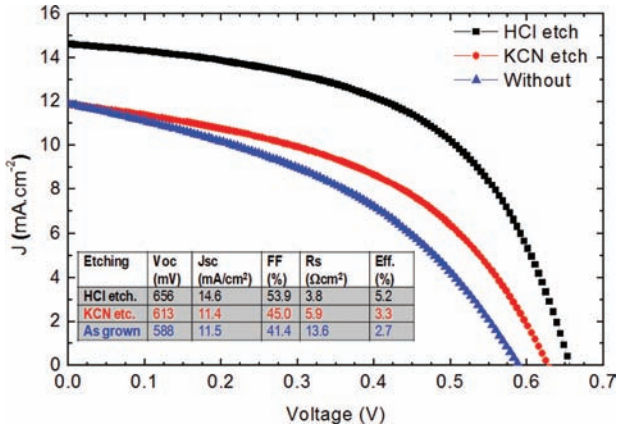

Etching	Voc (mV)	Jsc (mA/cm²)	FF (%)	Rs (Ωcm²)	Eff. (%)
HCl etch.	656	14.6	53.9	3.8	5.2
KCN etc.	613	11.4	45.0	5.9	3.3
As grown	588	11.5	41.4	13.6	2.7

Figure 3. Illuminated $J-V$ characteristics (AM1.5G filter, 100 mW/cm^2) of the solar cells prepared from the as-grown absorber, the absorber etched with KCN, and the absorber etched with HCl. Optoelectronic parameters have been extracted from these curves.

various samples, where the following average efficiencies were obtained: HCl treated, 9 samples, Eff. = 4.9 ± 0.3%; KCN treated, 6 samples, Eff. = 2.8 ± 0.5; and as grown, 6 samples, Eff. = 2.4 ± 0.3. As is clearly observed in Figure 3 and the corresponding table, this improvement is mainly related to those of the short-circuit current and the series resistance. These changes are directly related to the significant reduction of the content of the ZnS phase on the CZTS surface. The presence of this phase leads mainly to a degradation (increase) of the series resistance of the devices because of its high band gap, as has been previously suggested.[9]

The effectiveness of this etching process for Zn-rich phases (ZnSe) in CZTSe has not been studied as extensively as for the case of ZnS in CZTS. However, we have preliminary results to show that there is some reduction of the Zn and ZnSe signals as measured by XRF and Raman spectroscopy, albeit not as drastically as for ZnS. After etching in HCl (10% v/v, 75 °C, 600 s), the composition ratio Zn/Sn as measured by XRF changes from 1.53 to 1.34, and the intensity of the main ZnSe mode reduces ∼12% (see SI). Further optimization of the etching process, i.e., with different mineral acids, concentration, temperature, and etch time, may prove it to be ideal for CZTSSe films of varied S−Se content.

In summary, our preliminary results show the effectiveness of the proposed HCl-based etch for the selective removal of superficial Zn-rich secondary phases. This etching process has a significant impact on the optoelectronic parameters of the solar cells, markedly influencing the J_{sc} and R_s parameters and, consequently, the conversion efficiency of the devices. This opens the possibility for a customized process for CZTS technologies that is more environmentally friendly and considerably less toxic than the classical KCN etch. These results can be considered very important for the future industrial implementation of this low-cost technology.

■ ASSOCIATED CONTENT

Supporting Information

Experimental methods and characterization techniques. This material is available free of charge via the Internet at http://pubs.acs.org.

AUTHOR INFORMATION

Corresponding Author
esaucedo@irec.cat

Notes
The authors declare no competing financial interest.

ACKNOWLEDGMENTS

The research leading to these results has received funding from the People Programme (Marie Curie Actions) of the European Union's Seventh Framework Programme FP7/2007-2013/ under REA grant agreement no. 269167). The research was also partially supported by MINECO, project KEST-PV (ref. ENE2010-121541-C03-1). Authors from IREC and the University of Barcelona belong to the M-2E (Electronic Materials for Energy) Consolidated Research Group and the XaRMAE Network of Excellence on Materials for Energy of the "Generalitat de Catalunya". E.S. thanks the MINECO, Subprogram Ramón y Cajal (ref. RYC 2011-09212), and V.I.-R. thanks Subprogram Juan de la Cierva (ref. JCI-2011-10782).

REFERENCES

(1) Todorov, T.; Reuter, K. B.; Mitzi, D. B. *Adv. Mater.* **2010**, *22*, E156.
(2) Andersson, B. A. *Prog. Photovolt.: Res. Appl.* **2000**, *8*, 61.
(3) Wadia, C.; Alivisatos, A. P.; Kammen, D. M. *Environ. Sci. Technol.* **2009**, *43*, 2072.
(4) Persson, C. *J. Appl. Phys.* **2010**, *107*, 053710.
(5) Barkhouse, D. A. R.; Gunawan, O.; Gokmen, T.; Todorov, T. K.; Mitzi, D. B. *Prog. Photovolt.: Res. Appl.* **2011**, *20*, 6.
(6) Schubert, B.-A.; Marsen, B.; Cinque, S.; Unold, T.; Klenk, R.; Schorr, S.; Schock, H.-W. *Prog. Photovolt.: Res. Appl.* **2011**, *19*, 93.
(7) Redinger, A.; Berg, D. M.; Dale, P. J.; Siebentritt, S. *J. Am. Chem. Soc.* **2011**, *133*, 3320.
(8) Guo, Q.; Ford, G. M.; Yang, W.; Walker, B. C.; Stach, E. A.; Hillhouse, H. W.; Agrawal, R. *J. Am. Chem. Soc.* **2010**, *132*, 17384.
(9) Platzer-Björkman, C.; Scragg, J.; Flammersberger, H.; Kubart, T.; Edoff, M. *Sol. Energy Mater. Sol. Cells* **2012**, *98*, 110.
(10) Katagiri, H.; Jimbo, K.; Yamada, S.; Kamimura, T.; Maw, W. S.; Fukano, T.; Ito, T.; Motohiro, T. *Appl. Phys. Exp.* **2008**, *1*, 041201.
(11) Fontané, X.; Calvo-Barrio, L.; Izquierdo-Roca, V.; Saucedo, E.; Pérez-Rodriguez, A.; Morante, J. R.; Berg, D. M.; Dale, P. J.; Siebentritt, S. *Appl. Phys. Lett.* **2011**, *98*, 181905.
(12) Redinger, A.; Hönes, K.; Fontané, X.; Izquierdo-Roca, V.; Saucedo, E.; Valle, N.; Pérez-Rodríguez, A.; Siebentritt, S. *Appl. Phys. Lett.* **2011**, *98*, 101907.
(13) Weber, M.; Scheer, R.; Lewerenz, H. J.; Jungblut, H.; Störkel, U. *J. Electrochem. Soc.* **2002**, *149*, G77.
(14) Weinhardt, L.; Fuchs, O.; Groß, D.; Umbach, E.; Heskeb, C.; Dhere, N. G.; Kadam, A. A.; Kulkarni, S. S. *J. Appl. Phys.* **2006**, *100*, 024907.
(15) Timmo, K.; Altosaar, M.; Raudoja, J.; Grossberg, M.; D'Anilson, M.; Volobujeva, O.; Mellikov, E. Proceedings of the 35th IEEE Photovoltaic Specialists Conference, Honolulu, HI, 2010; 001982.
(16) Timmo, K.; Altosaar, M.; Raudoja, J.; Volobujeva, O.; Kauk, M.; Krustok, J.; Varema, T.; Grossberg, M.; Danilson, M.; Muska, K.; Ernits, K.; Lehner, F.; Meissner, D. *Mater. Challenges Alternative Renewable Energy: Ceramic Trans.* **2011**, *224*, 137.
(17) Maeda, K.; Tanaka, K.; Fukui, Y.; Uchiki, H. *Sol. Energy Mater. Sol. Cells* **2011**, *95*, 2855.
(18) Scragg, J.; Berg, D.; Dale, P. *J. Electroanal. Chem.* **2010**, *646*, 52.
(19) Lauermann, I.; Bär, M.; Fischer, C.-H. *Sol. Energy Mater. Sol. Cells* **2011**, *95*, 1495.
(20) Li, X.; Wang, D.; Du, Q.; Liu, W.; Jiang, G.; Zhu, Ch. *Adv. Mater. Res.* **2012**, *418−420*, 67.